Toward the Design of an RNA:DNA Hybrid Binding Agent

Wenhua Chu, Shigehiro Kamitori, Miho Shinomiya, Robert G. Carlson, and Fusao Takusagawa*

Contribution from the Departments of Chemistry and Biochemistry, University of Kansas, Lawrence, Kansas 66045-0046

Received July 14, 1993®

Abstract: One characteristic function of the retroviruses, which is generally not found in normal eukaryotic cells, is production of a long RNA:DNA hybrid in the viral replication phase. If agents are designed which bind only to the RNA:DNA hybrid, but neither to DNA nor to RNA, such agents will be able to inhibit specifically the RNase H activity of retroviral reverse transcriptase, and therefore will suppress viral replication. Actinomycin D binds to double-stranded DNA, but not to RNA, because steric hindrance between the 2-amino group of the phenoxazinone ring and the 2′-hydroxyl group of RNA prevents intercalation of the antibiotic. However, if the C8-H in the phenoxazinone ring is replaced by an aromatic nitrogen N8, a strong hydrogen bond acceptor, this analog (N8-actinomycin D) might be able to bind intercalatively to an RNA:DNA hybrid by forming an additional hydrogen bond between N8 and the 2′-hydroxyl group of guanosine ribose. This hypothesis has been tested by a molecular mechanics calculation using a model structure of the complex between N8-actinomycin D and a small RNA:DNA hybrid, r(GC):d(GC). The results of the molecular mechanics calculation suggest that N8-actinomycin D can intercalatively bind to the RNA:DNA hybrid by making an additional intracomplex hydrogen bond. This hydrogen bonding capability of N8 has been confirmed in the crystal structure of the chromophore of N8-actinomycin D. Thus, N8-actinomycin D has been synthesized by coupling the pyridine and benzene fragments obtained independently. A binding study indicates that both actinomycin D and N8-actinomycin D bind intercalatively not only to DNA;DNA double strands but also to RNA:DNA hybrids. Although the overall binding capacity of N8-actinomycin D is reduced substantially in comparison with that of actinomycin D itself, N8-actinomycin D tends to bind relatively more favorably than actinomycin D to the RNA:DNA hybrids. Thus, this initial attempt at designing an RNA:DNA hybrid binding agent appears to be successful. However, it is necessary to modify the agent further to increase its RNA:DNA hybrid binding character and to decrease the DNA:DNA binding character, in order to make a useful RNA:DNA hybrid binding agent.

Introduction

Acquired immunodeficiency syndrome (AIDS), caused by the retrovirus HIV, is currently a serious medical problem. Retroviruses may also participate in the pathogenesis of certain cancers.[1,2] The viral enzyme reverse transcriptase makes a minus-strand DNA copy of viral RNA. This enzyme is characteristic for the family of retroviruses but is generally not found in normal eukaryotic cells. Thus, interferences with various actions of reverse transcriptase are potential approaches to the therapy of HIV infection (AIDS). *In vivo*, HIV reverse transcriptase uses a lysine transfer RNA as a primer to make a minus-strand DNA copy of the viral RNA as an RNA:DNA hybrid,[3] Besides having reverse transcriptase activity, the enzyme possesses an inherent RNase H activity that specifically degrades the RNA of the RNA:DNA hybrid.[4-9] Therefore, in theory, inhibition of this process would suppress the viral replication. Thus, we are looking for agents that bind only to the RNA:DNA hybrid, but neither to double-stranded DNA nor to RNA. Such agents would specifically inhibit the RNase H activity of reverse transcriptase and, therefore, suppress viral replication.

Biological studies have indicated that actinomycin D (AMD), shown in Figure 1, moderately inhibits reverse transcriptase activity.[10,11] *In vitro*, a 50% inhibition of reverse transcriptase activity is reached at a 35 μg/mL concentration of AMD, while a 50% inhibition of RNA polymerase activity is reached at a 1.5 μg/mL concentration of AMD.[10] The experimental data obtained from the inhibition of reverse transcriptase activity by the ribonuclease and AMD suggest that the antibiotic does not inhibit the synthesis of the RNA:DNA hybrid using viral RNA as a template, but does inhibit the subsequent synthesis of double-stranded DNA, and the inhibited reaction synthesizes low molecular weight double-stranded DNA.[11] These experimental results suggest that the AMD might bind intercalatively on the RNA:DNA hybrid, and the agent inhibits the RNase H activity of retroviral reverse transcriptase.

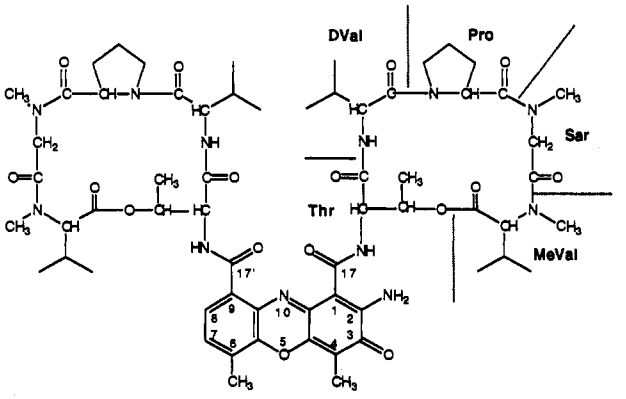

Figure 1. Molecular structure of actinomycin D (AMD).

Studies by dialysis,[12] electrophoresis,[13] ultracentrifugation,[14] and chromatography on Sephadex[15] indicated that AMD can

* Abstract published in *Advance ACS Abstracts*. February 15, 1994.

(1) Gallo, R. C. *Sci. Am.* **1986**, *255*, 88–98.
(2) Gallo, R. C. *Sci. Am.* **1987**, *256*, 47–56.
(3) Wain-Holson, S.; Sonigo, P.; Danos, O.; Cole, S.; Alizon, M. *Cell* **1985**, *40*, 9–17.
(4) Swanstorm, R.; Varmus, H. E.; Bishop, J. M. *J. Biol. Chem.* **1981**, *256*, 1115–1121.
(5) Resnick, R.; Omer, C. A.; Faras, A. J. *J. Virol.* **1984**, *51*, 813–821.
(6) Omer, C. A.; Faras, A. J. *Cell.* **1982**, *30*, 797–805.
(7) Gerard, G. F. *Biochemistry* **1981**, *20*, 256–264.
(8) Champoux, J. J.; Gilboa, E.; Baltimore, D. *J. Virol.* **1984**, *49*, 686–691.
(9) Verma, I. M. *Biochim. Biophys. Acta* **1977**, *473*, 1–38.
(10) Müller, W. E. G.; Zahn, R. K.; Seidel, H. J. *Nat. New Biol.* **1971**, *232*, 143–145.
(11) McDonnell, J. P.; Quintrell, N.; Garapin, A.-C.; Fanshier, L.; Levinson, W. E.; Bishop, J. M. *Nature* **1970**, *228*, 433–435.
(12) Kirk, J. M. *Biochim. Biophys. Acta* **1960**, *42*, 167–169.
(13) Kawamata, J.; Imanishi, M. *Biken J.* **1961**, *4*, 13–24.

0002-7863/94/1516-2243$04.50/0

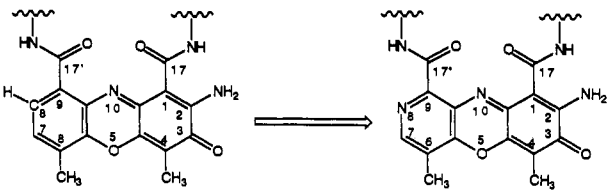

Figure 2. Modification of actinomycin D (AMD) to N8-actinomycin D (N8AMD). The C8-H in the phenoxazinone ring is changed to N8.

bind to DNA, but not to RNA, with a preference for the 5′-GC sequence.[16] A recent X-ray crystallographic study[17] and a 2-D NMR study[18] on complexes between AMD and a small piece of DNA show how the drug interacts with DNA. An examination of the structure shows why AMD cannot bind to RNA.[17-19] The 2′-hydroxyl group of the ribose would have unusually short contacts with the 2-amino group of the phenoxazinone ring, if the deoxyribose of the guanosine is changed to ribose. This would also be the case in an intercalated model in which the distance, C2′···N2, is already quite short;[20] it would thus be clearly impossible to replace the guanosine deoxyribose by ribose. However, if the C8-H of the phenoxazinone ring is replaced by the strong hydrogen bond acceptor N8 (Figure 2), the 2′-hydroxyl group of the guanosine ribose (RNA) will be able to make a hydrogen bond to N8 as illustrated in Figure 3. A preliminary molecular modeling study on a complex between a piece of RNA:DNA hybrid, r(GC):d(GC), and the AMD analog (N8AMD) suggests that it is possible to form an additional hydrogen bond between the 2-hydroxyl group and N8 of 8-azaphenoxazinone ring. The interaction energy between the drug and the nucleic acid in the RNA:DNA hybrid complex would be larger than that in the DNA:DNA complex, because of an additional hydrogen bond between the drug and the RNA:DNA hybrid. Furthermore, the presence of N8, which strongly hydrogen-bonds to the solvent (water), would reduce substantially the intercalation capability of the N8AMD to DNA:DNA double strands (but hopefully not to RNA:DNA hybrids). For testing our hypothesis, we have actually synthesized N8AMD and examined the binding character of the agent to nucleic acids.

Results and Discussion

Molecular Modeling Study. Four simple models of dinucleoside phosphate–drug complexes have been built from the crystal structures of the DNA–AMD complex.[17] Those are (1) [r(GC):d(GC)]–N8AMD, (2) [r(GC):d(GC)]–AMD, (3) [d(GC):d(GC)]–N8AMD, and (4) [d(GC):d(GC)]–AMD.

The model structures were refined by a molecular mechanics method using the program AMBER.[22] Since the model system used here is very simple and solvent effects are completely omitted in the calculation, calculated force field energies are not reliable enough quantities to use to estimate the binding constants of the agents either to the RNA:DNA hybrids or to DNA:DNA double strands. However, the interaction energies between the drugs and the dinucleosides may indicate degrees of stability of the complexes (Table 1). The complex of [r(GC):d(GC)]–N8AMD

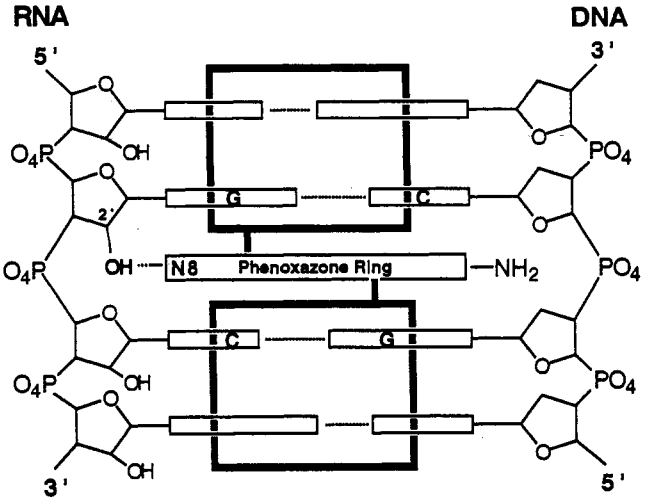

Figure 3. Schematic view of the N8-actinomycin D binding site on the RNA:DNA hybrid. The important O2′-H···N8 hydrogen bond is shown by a dotted line.

Table 1. Interaction Energies between Dinucleoside Phosphate and N8AMD or AMD (kcal/mol)

(1) [r(GC):d(GC)]–N8AMD	−55.09
(2) [r(GC):d(GC)]–AMD	−52.30
(3) [d(GC):d(GC)]–N8AMD	−54.54
(4) [d(GC):d(GC)]–AMD	−52.13

has the largest interaction energy among the four complex systems, although differences of interaction energies are very small. In the structure of [r(GC):d(GC)]–N8AMD (Figure 4), the 2′-hydroxyl group of the guanosine ribose indeed makes an additional intracomplex hydrogen bond (H···N = 1.921 Å) with N8 of the 8-azaphenoxazinone ring. This suggests that N8AMD might bind preferentially to RNA:DNA hybrids. All four complex structures refined by a molecular mechanics calculation show that the chromophores stay in the intercalated mode between the GC base pairs without any unusual short contacts with the nucleoside phosphate backbone. The four strong hydrogen bonds between threonine residues and guanine bases bind the AMD or N8AMD to the dinucleoside phosphate duplex as found in the crystal structures[17,19] and 2-D NMR structure.[18] In addition to these hydrogen bonds, the 2-amino hydrogen H(N2) of the chromophore makes a hydrogen bond to O4′ of the cytosine deoxyribose.

Synthetic Study. Several total synthetic schemes of AMD have been reported and reviewed.[23,24] The preferred route to synthetic AMD is to synthesize each half of the molecule with the cyclic depsipeptide in place. Thus, a similar synthetic scheme has been examined to synthesize N8AMD. Initially one half of the chromophore, methyl 1,4-dihydro-3-amino-5-methyl-4-oxo-2-pyridinecarboxylate (**12**), was synthesized from 2,5-dimethylpyridine. The other half of the chromophore, methyl 2-amino-3-hydroxyl-4-methylbenzoate (**13**), was obtained from 3-hydroxyl-4-methyl-2-nitrobenzoic acid. Dimethyl 2-amino-4,6-dimethyl-3-oxo-8-azaphenoxazine-1,9-dicarboxylate (**14a**), the chromophore of N8AMD, was then synthesized by coupling the two fragments as shown in Scheme 1. This initial synthetic work suggested not only a possible synthetic route to N8AMD but also the favorable hydrogen bonding character of N8, which will be described in the crystal structure of the chromophore. Of particular interest is that no nitration occurred at the 3-position of pyridine when the 2-methyl group was oxidized first to CH_2OH in step 4. In the

(14) Rauen, H. M.; Kersten, H.; Kersten, W. *Z. Physiol. Chem.* **1960**, *321*, 139–147.
(15) Hartmann, G.; Coy, U.; Kniese, G. *Z. Physiol. Chem.* **1962**, *330*, 227–233.
(16) Cerami, A.; Reich, E.; Ward, D. C.; Goldberg, I. H. *Proc. Natl. Acad. Sci. U.S.A.* **1967**, *57*, 1036–1042.
(17) Kamitori, S.; Takusagawa, F. *J. Mol. Biol.* **1992**, *225*, 445–456.
(18) Liu, X.; Chen, H.; Patel, D. J. *J. Biomol. NMR* **1991**, *1*, 323–347.
(19) Takusagawa, F.; Dabrow, M.; Neidle, S.; Berman, H. M. *Nature* **1982**, *296*, 466–469.
(20) Sobell, H. M.; Jain, S. C. *J. Mol. Biol.* **1972**, *68*, 21–34.
(21) Müller, W.; Crothers, D. M. *J. Mol. Biol.* **1968**, *35*, 251–290.
(22) Pearlman, D. A.; Case, D. A.; Caldwell, J. C.; Seibel, G. L.; Singh, U. C.; Weiner, P.; Kollman, P. A. *AMBER: Assisted Model Building with Energy Refinement. A general program for modeling molecules and their interactions*, Version 4.0; UCSF, 1991. Mauger, A. B. The actinomycins. In *Topics in Antibiotic Chemistry*; Sammes, P. G., Ed.; E. Horwood: Chichester, U.K., 1980; pp 224–306.
(23) Meienhofer, J.; Atherton, E. Structure-Activity Relationships in the Actinomycins. In *Structure-Activity Relationships among the Semisynthetic Antibiotics*; Perlman, D., Ed.; Academic Press: New York, San Francisco, London, 1974; pp 427–529.
(24) Mauger, A. B.; Stuart, O. A.; Ferretti, J. A.; Silverton, J. V. *J. Am. Chem. Soc.* **1985**, *107*, 7154–7163. Mauger, A. B.; Stuart, O. A.; Katz, E. *J. Med. Chem.* **1991**, *34*, 1297–1301.

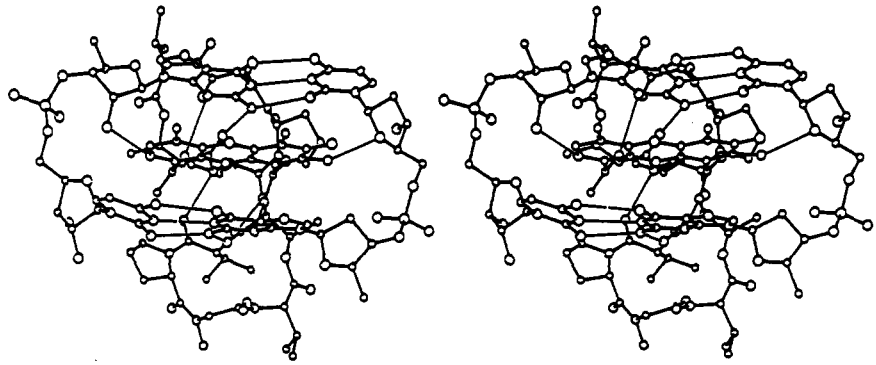

Figure 4. Stereoscopic view of the [r(GC):d(GC)]–N8AMD complex structure refined by a molecular mechanics calculation (AMBER). All hydrogen atoms and O5′ of guanosine are omitted in order to simplify the figure. The thin lines represent hydrogen bonds. The r(GC) in the hybrid structure is located at the left side of the duplex.

Scheme 1. Syntheses of the Pyridine Fragment (**12**) and Chromophore of N8AMD (**14**)[a]

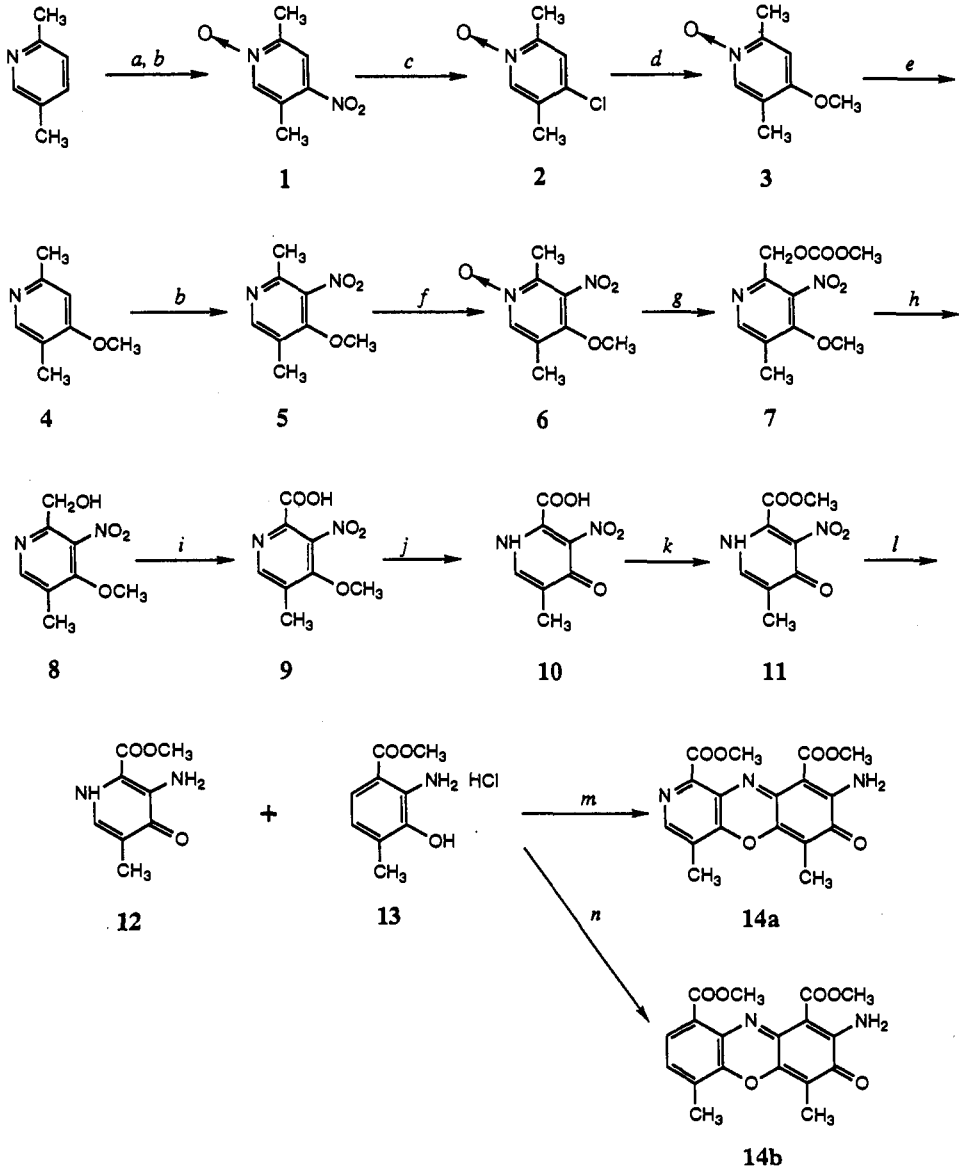

[a] (*a*) H_2O_2, CH_3COOH; (*b*) HNO_3, H_2SO_4; (*c*) CH_3COCl; (*d*) CH_3ONa; (*e*) PCl_3; (*f*) MCPBA; (*g*) $(CH_3CO)_2O$; (*h*) KOH; (*i*) $KMnO_4$, Na_2CO_3; (*j*) HBr; (*k*) CH_3OH, HCl; (*l*) Pd/C, H_2; (*m*) $K_3Fe(CN)_6$ at pH 4.75; (*n*) $K_3Fe(CN)_6$ at pH 7.12. The abbreviation MCPBA = *m*-chloroperbenzoic acid.

coupling reaction between the pyridine and benzene fragments, the final product (**14a**) formed only when a solution of **13** was added drop by drop to a solution of **12** at pH 4.75. When equal amounts of **12** and **13** solutions at pH 7.0 were mixed together with $K_3Fe(CN)_6$, **13** coupled only with itself to give the chromophore of AMD (**14b**).

The cyclic depsipeptide (**19**) has been synthesized by a slight modification of the method described by Mauger,[24] and the procedure is given in Scheme 2. It should be noted that the method developed by Nakajima *et al.*,[25] by which we first tried to synthesize the cyclic depsipeptide (**19**), gave the ring containing the *N*-methyl-D-valine (**19′**) instead of the *N*-methyl-L-valine. A

Scheme 2. Synthesis of Cyclic Depsipeptide **19**[a]

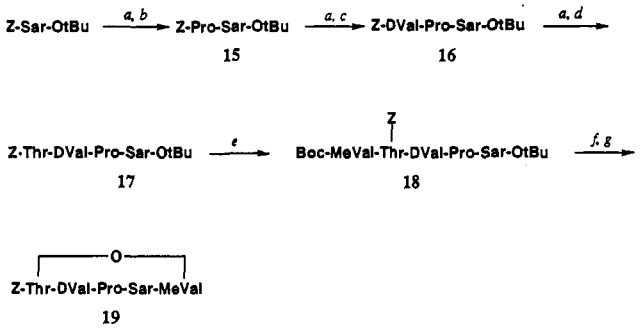

[a] (*a*) Pd/C, H_2; (*b*) Z-Pro, DCC; (*c*) Z-DVal, DCC; (*d*) Z-Thr, DCC; (*e*) Boc-MeVal, DMAP, DCC; (*f*) F_3CCOOH; (*g*) BOP-Cl, Et_3N. Abbreviations used are Boc = *N-tert*-butoxycarbonyl; BOP-Cl = *N,N*-bis(2-oxo-3-oxazolidinyl)phosphorodiamidic chloride; DCC = dicyclohexylcarbodiimide; DMAP = 4-(dimethylamino)pyridine; Z = 3-(benzyloxy)-4-methyl-2-nitrobenzoyl.

Scheme 3. Synthesis of N8AMD (**24**)[a]

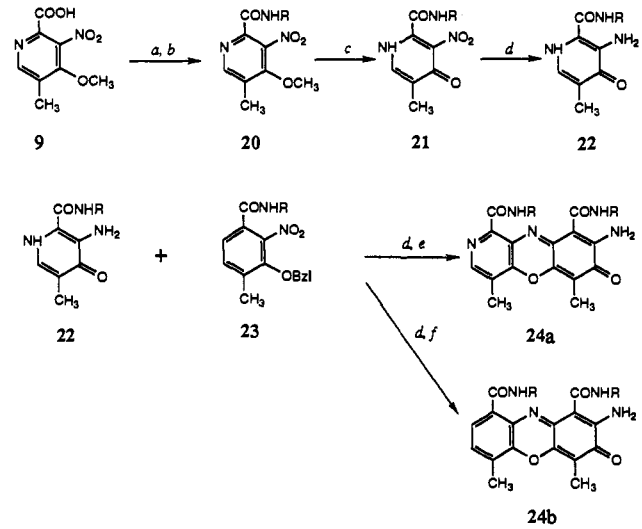

[a] (*a*) **19**, Pd/C, H_2; (*b*) DCC; (*c*) BBr_3; (*d*) Pd/C, H_2; (*e*) $K_3Fe(CN)_6$ at pH 4.75; (*f*) $K_3Fe(CN)_6$ at pH 7.1. The abbreviation R = -Thr-DVal-Pro-Sar-MeVal.

large portion of the L-form of *N*-methylvaline appears to be converted to the D-form of *N*-methylvaline in the coupling reaction of Boc-Sar-MeVal-OH and Z-3-MeAzy-D-Val-Pro-OtBu. This unexpected reaction was confirmed by determining the crystal structure of the cyclic depsipeptide (**19′**) as shown in Figure 7. The optical rotation $[\alpha]^{23}_D$ of the correct compound (**19**) is −31.6°, which is clearly different from +21.6° of the "wrong" cyclic depsipeptide (**19′**).

The final product N8AMD (**24a**) was synthesized by coupling of the two halves of the molecule with the cyclic depsipeptide in place as shown in Scheme 3. One half of the molecule, the pyridine fragment (**22**), was obtained by coupling 4-methoxy-5-methyl-3-nitropyridine-2-carboxylic acid (**9**) and the cyclic depsipeptide (**19**). The other half of the molecule, the benzene fragment (**23**), was synthesized from 3-hydroxy-4-methyl-2-nitrobenzoic acid and the cyclic depsipeptide (**19**). In the coupling reaction between the pyridine and benzene fragments, the same procedure used in the synthesis of the chromophore was applied. As a byproduct, AMD (**24b**) was also synthesized and was found spectrometrically to be identical with the natural compound.

X-ray Crystallography Study. The crystal structures of compounds **12** and **14a** have been determined to confirm their structures (Figure 5). The crystal structure of **12** shows that the molecule adopts a keto form, suggesting that coupling reaction

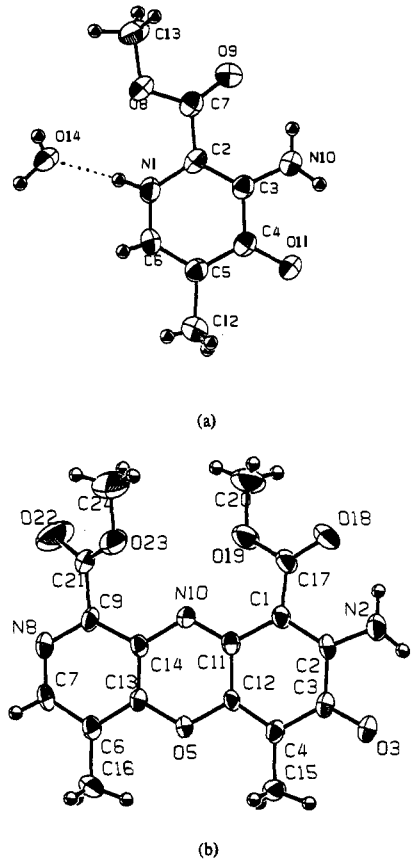

Figure 5. Molecular structures of compounds **12** (a) and **14a** (b) determined by the X-ray analysis. The molecule of **12** adopts a keto form, in which the pyridine nitrogen is protonated and the ring takes quinone form.

between **12** and **13** should take place only at a lower pH. In fact, **13** coupled with **12** only at lower pH (pH 4.7) to give the 8-azaphenoxazinone ring (**14a**). At pH 7.0, **13** coupled with itself to give the chromophore of AMD (**14b**).

As discussed in the previous section (Molecular Modeling Study), the N8 in the 8-azaphenoxazinone ring is required to participate in a hydrogen bond if N8AMD binds strongly to the RNA:DNA hybrid. The results of X-ray analysis of compound **14a** provided us not only confirmation of the coupling reaction but also strong support of our hypothesis that the N8 becomes a favorable hydrogen bond acceptor of the 2′-hydroxyl group of RNA. In the crystal structure of **14a** (Figure 6), the N8 is indeed a hydrogen bond acceptor of the 2-amino hydrogen. It should be noted that the N8 is a quite favorable hydrogen bond acceptor in comparison with other possible hydrogen bond acceptors such as O3, O5, N10, O18, O19, O22, and O23. A similarly strong hydrogen bonding character of aromatic nitrogen atoms has been found between crystal structures of isoelectronic benzenecarboxylic acids and pyridinecarboxylic acids.[26] In the structures of pyridinecarboxylic acids, the ring nitrogen atoms participate in hydrogen bonds with no exceptions, whereas several carbonyl oxygen atoms are free from hydrogen bonds.

As discussed in the previous section, crystal structures of two cyclic depsipeptides (**19′** and **20**) have been determined in order to confirm their structures. Although the absolute configurations of *N*-methylvalines in compounds **19′** and **20** are opposite from each other, both cyclic depsipeptides adopt a very similar rectangular backbone conformation, as shown in Figure 7. All cyclic depsipeptides that have been found in AMD,[27] DNA–AMD complexes,[17-20] and an AMD analog[24] are also quite similar

(25) Nakajima, K.; Tanaka, T.; Neya, M.; Okawa, K. *Bull. Chem. Soc. Jpn.* **1982**, *55*, 3237–3241.

(26) Takusagawa, F.; Hirotsu, K.; Shimada, A. *Bull. Chem. Soc. Jpn.* **1973**, *46*, 2020–2027.

(27) Ginell, S.; Lessinger, L.; Berman, H. M. *Biopolymers* **1988**, *27*, 843–864.

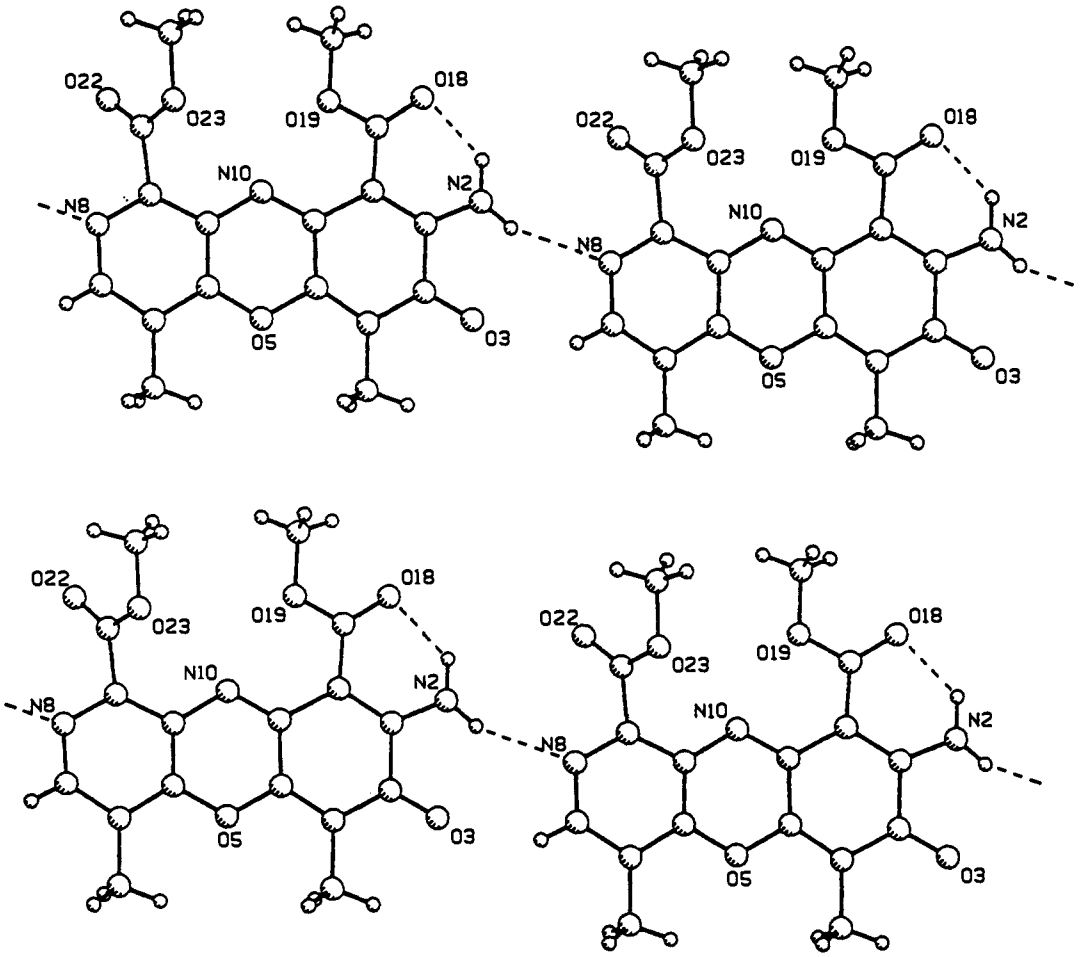

Figure 6. View of the crystal structure of **14** down the [1,0,−1] direction, showing the molecular packing and the hydrogen bonding network (N2-H···N8: N2···N8 = 3.111(6) Å, H···N8 = 2.29(5) Å, ∠N2-H···N8 = 155(5)°; N2-H···O18: N2···O18 = 2.645(6) Å, H···O18 = 1.91(5) Å, ∠N2-H···O18 = 134(5)°) in a layer. In the crystal structure, these layers are stacked with a spacing of 3.357 Å and are related to each other by *c*-glide symmetries.

to those of **19′** and **20**. These crystallographic results suggest that the configuration of *N*-methylvaline does not influence the backbone conformation of the cyclic depsipeptide, but the other four amino acid residues appear to be crucial to form a rigid 16-membered ring. The proline and sarcosine whose nitrogen atoms are blocked with hydrophobic groups are essential to change the peptide bond to *cis*- from the normal *trans*-linkage, and the threonine is required to make a lactone linkage. If the D-valine is replaced with the L-valine, the isopropyl group will point into the ring (see Figure 7). As pointed out by Takusagawa,[28] the unique amino acid sequence of AMD has been chosen by microorganisms in order to build a rigid peptide ring to play an important role in the inhibition of the RNA polymerase activity.

Binding Study. A DNA:DNA double strand, RNA:DNA hybrid, and DNA and RNA single strands, all with the drug-binding site 5′-GC-3′ in the middle, utilized to examine the binding characteristics of N8AMD and AMD are shown below. In order

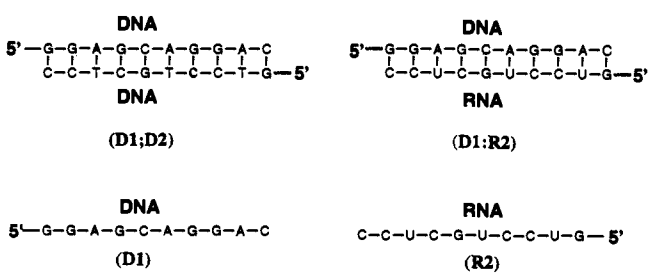

to prevent melting of the double-stranded DNA:DNA and RNA:DNA, the G/C rich sequences have been selected, and the spectra have been measured at relatively high salt condition (300 mM of NaCl). Since the visible spectrum (350–500 nm) of the chromophore is slightly shifted to the longer wavelength region (red shift) by the drug intercalating into the nucleic acid, the difference spectrum between the drug itself and the drug–nucleic acid complex should resemble a negative sine curve, if the chromophores of drugs stacked with the bases or base pairs of oligonucleotides.

It is necessary to determine whether the non-self-complementary DNA:DNA and RNA:DNA hybrids stay double strands in solution. This was confirmed by measuring the melting point spectra and comparing the spectra between the double and single strands. As shown in Figure 8, the DNA:DNA and RNA:DNA double strands start to melt around 25 °C, whereas the single-strand DNA does not show any melting behavior. This indicates that major portions of the non-self-complementary DNA mixture, d(GGAGCAGGAC):d(GTCCTGCTCC), and the RNA:DNA hybrid mixture, d(GGAGCAGGAC):r(GUCCUGCUCC) stay in double-stranded form below 20 °C. Therefore the binding experiment was carried out at 18 °C.

The visible spectra were measured at four different DNA concentrations (0, 2, 4, and 6 μM) in the drug solution (10 μM), namely drug:DNA ratios of 10:0, 10:2, 10:4, and 10:6, respectively, in order to estimate the constants for binding of drugs to oligonucleotides. Difference spectra of N8AMD (**24a**) and AMD (**24b**) with DNA:DNA double strands, RNA:DNA hybrids, and DNA single strands are given in Figures 9 and 10. These spectra show clearly that both AMD and N8AMD bind intercalatively not only to the DNA:DNA double strands but also to the RNA:

(28) Takusagawa, F. *J. Antibiot.* **1985**, *38*, 1596–1604.
(29) Salazar, M.; Fedoroff, O. Y.; Miller, J. M.; Ribeiro, N. S.; Reid, B. R. *Biochemistry* **1993**, *32*, 4207–4215.

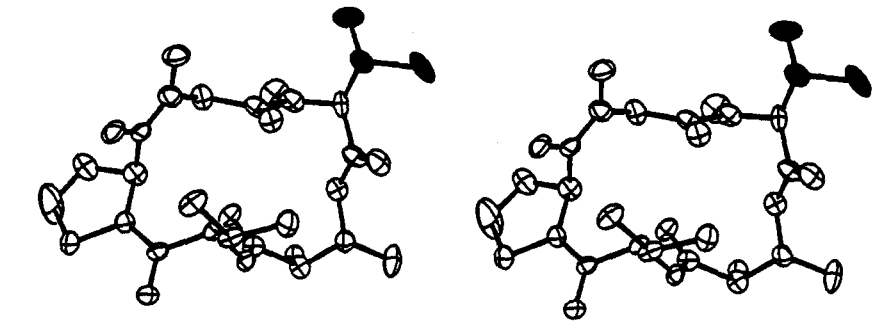

(a)

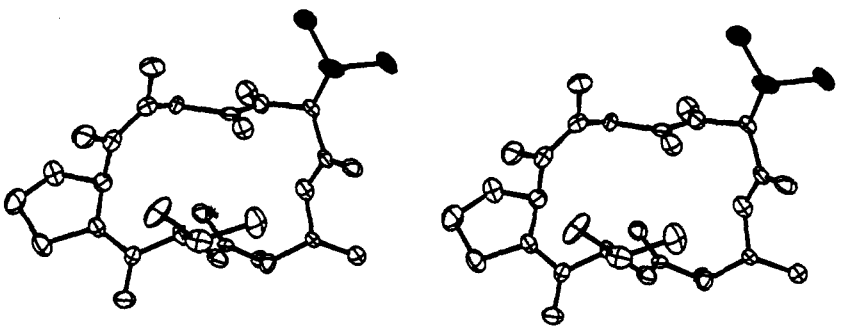

(b)

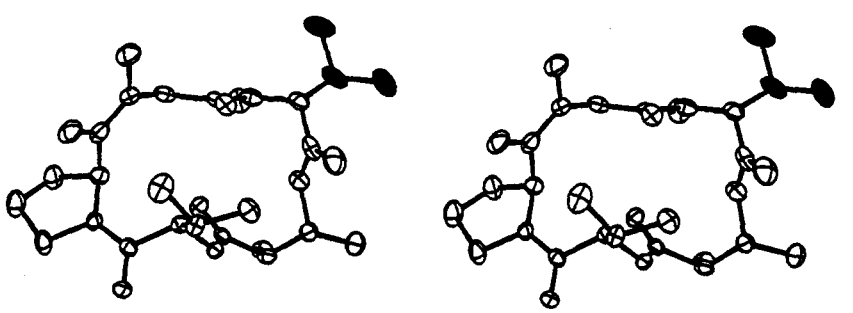

(c)

Figure 7. Stereoviews of cyclic depsipeptides of compound **20** (a and b) and **19'** (c), showing quite similar rectangular confirmations of the rings. A wrong configuration (D-form instead of L-form) of methylvaline was found in the cyclic depsipeptide of **19'** (c) synthesized by the method described by Nakajima *et al.*[25] The isopropyl group of *N*-methyl-D-valine is marked with solid circles.

DNA hybrids. Since AMD does bind to the RNA:DNA hybrid, this result supports the earlier observation,[11] in which AMD inhibits the reverse transcriptase activity in synthesis of the double-stranded DNA from the RNA:DNA hybrid but does not inhibit the synthesis of the RNA:DNA hybrid from a single RNA strand. It should be noted that several old experimental data,[30] which suggested that AMD does not bind to the RNA:DNA hybrid, appear to have been misinterpreted. The difference spectra show that both AMD and N8AMD bind quite strongly to the DNA single strands, whereas the drugs do not bind to the single-strand RNA.

If the drug spectrum is simply shifted by $\Delta\lambda$ and the magnitude of its absorbance is proportionally changed by S when the drug intercalates into the oligonucleotides, then the absorbance of the complex at the wavelength of λ should be represented as $SA_d(\lambda - \Delta\lambda)$. The calculated spectrum $A_c(\lambda)_{cal}$ of the drug–oligonucleotide mixture, whose noncomplex and complex contents are $(1 - \alpha)$ and α, respectively, is represented as a sum of $A(\lambda)$ and $SA(\lambda - \Delta\lambda)$, *i.e.*

$$A_c(\lambda)_{cal} = (1 - \alpha)A_d(\lambda)_{obs} + \alpha SA_d(\lambda - \Delta\lambda)_{obs} \quad (1)$$

(30) Müller, W. *Naturwissenschaften* **1962**, *49*, 156–157.
(31) Waring, M. J. Inhibitors of Nucleic Acid Synthesis. In *The Molecular Basis of Antibiotic Action*; (Gale, F., *et al.*, Eds.; John Wiley & Sons: London, New York, Sydney, Toronto, 1980; pp 258–401.

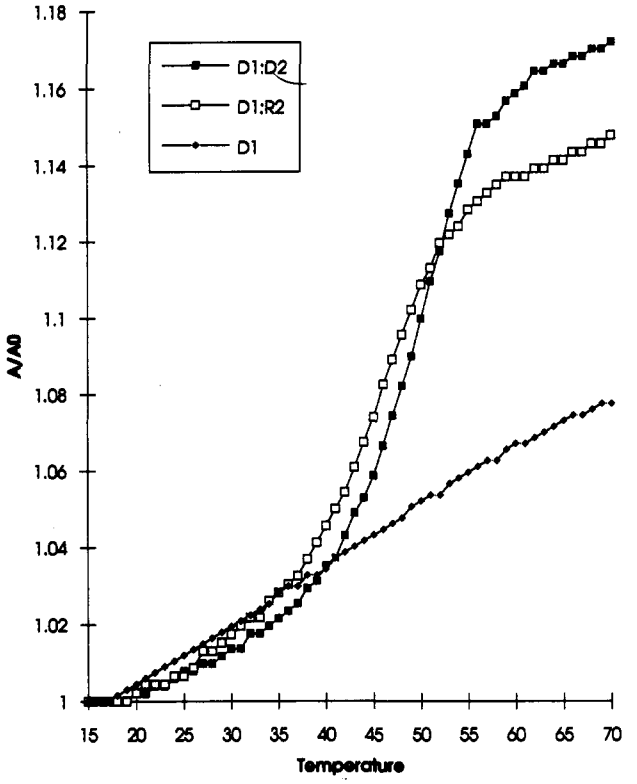

Figure 8. D1:D2, D1:R2, and D2 melting point spectra. The absorbances at 260 nm were measured from 15 to 70 °C by 1 °C steps. The oligonucleotides were in 20 mM phosphate buffer (pH 7.0) containing 300 mM NaCl. D1 = d(GGAGCGGAC); D2 = d(GTCCGCTCC); R2 = r(GUCCGCUCC).

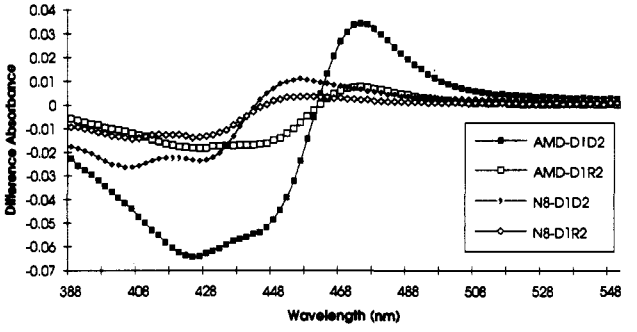

Figure 9. Difference spectra of AMD–(D1:D2), AMD–(D1:R2), N8AMD–(D1:D2), and N8AMD–(D1:R2) at oligonucleotide and drug concentrations of 2 and 10 μM, respectively.

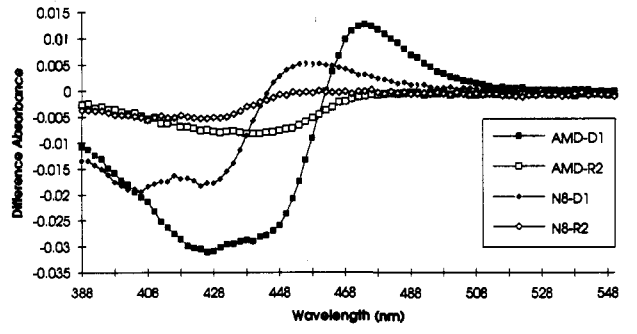

Figure 10. Difference spectra of AMD–(D1), AMD–(R2), N8AMD–(D1), and N8AMD–(R2) at oligonucleotide and drug concentrations of 2 and 10 μM, respectively.

where $A_d(\lambda)_{obs}$ and $A_d(\lambda - \Delta\lambda)_{obs}$ are the observed absorbance of the drug at λ and $\lambda - \Delta\lambda$ wavelengths, respectively. $\Delta\lambda$, α, and S have been determined by minimizing $\sum[A_c(\lambda)_{obs} - A_c(\lambda)_{cal}]^2$. The difference spectra calculated from the observed $A_c(\lambda)_{obs}$ and calculated $A_c(\lambda)_{cal}$ are in good agreement to each other as shown

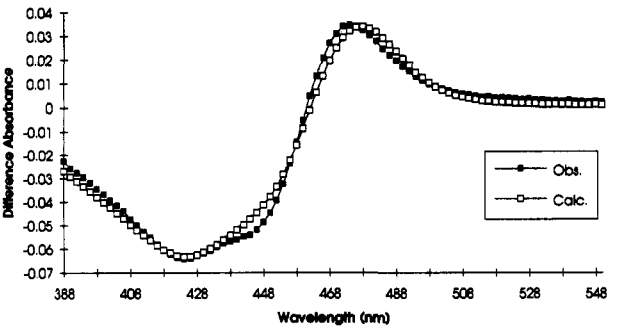

Figure 11. Observed and calculated difference spectra of AMD–(D1:D2) at D1:D2 and drug concentrations of 2 and 10 μM, respectively.

Table 2. Binding Constants (M^{-1}) of AMD and N8AMD to Various Oligonucleotides

drug	oligonucleotide[a]	k_a	S	$\Delta\lambda$ (nm)
AMD	D1:D2	2.7×10^6	0.63	20
AMD	D1:R2	3.4×10^4	0.58	20
AMD	D1	1.0×10^5	0.61	22
N8AMD	D1:D2	3.9×10^4	0.56	40
N8AMD	D1:R2	1.6×10^4	0.47	40
N8AMD	D1	3.2×10^4	0.49	40

[a] D1 = d(GGAGCAGGAC), D2 = d(GTCCTGCTCC), R2 = r(GUCCUGCUCC).

in Figure 11. From α, drug concentration (C), and the ratio of the oligonucleotide and the drug (R), the binding constant, k_a, is

$$k_a = \alpha/[(1 - \alpha)(R - \alpha)C] \quad (2)$$

The three binding constants obtained at three different oligonucleotide ratios (0.2, 0.4, and 0.6) should agree with each other if the above assumption is correct. The K_a at low oligonucleotide ratio ($R = 0.2$) is always larger than the K_a at a high concentration ($R = 0.6$). Especially the α value of the AMD–DNA:DNA complex at a 0.065 DNA ratio becomes as large as three times the R value, and subsequently the K_a becomes negative. This observation suggests that three drugs appear to bind to one DNA:DNA, *i.e.*, one drug intercalates to the middle of the DNA and the other two drugs stack on the G≡C base pairs of both ends of the DNA. When the DNA concentration is increased to several times the drug concentration, only one drug binds to the DNA:DNA. Thus, a correction function, y, which is a simple Gaussian function of R, is applied to correct the α value.

$$y = 2\exp(-xR^2) + 1$$

The best x value has been determined by minimizing $\sum(K_{ai} - K_{aj})^2$, where K_{ai} and K_{aj} are the binding constants of different DNA ratios. The y value becomes 1.0 when the R value goes to 1 or higher, suggesting the major binding site of the drug is the intercalation sequence, 5′-GC-3′. Although the new K_a obtained by this procedure should be somewhat underestimated, the mean value $\langle k_a \rangle$, 2.7×10^6 M^{-1}, from six different measurements (0,065 < R < 1.0) of AMD–DNA:DNA, is in quite good agreement with the literature value,[21] 2.3×10^6 M^{-1}.

The binding constants of AMD and N8AMD to the oligonucleotides are listed along with S and $\Delta\lambda$ in Table 2. The scale factors, S, and shift wavelengths, $\Delta\lambda$, of AMD and N8AMD are significantly different from each other. Absorption spectra of AMD are shifted by 20 nm and reduced to 63% when the drug intercalates into the nucleic acid, while the corresponding numbers for the N8AMD–nucleic acid complex are 40 nm and 56% as listed in Table 2. Although the S and $\Delta\lambda$ of AMD obtained by this study cannot quantitatively compare with the changes in the visible spectrum of AMD, they are relatively in good agreement with each other. For instance, for the binding to calf thymus DNA measured spectrophotometrically by the bathochromic shift,

$\Delta\lambda$, and the change in extinction, $\Delta\epsilon_{max}$, the values are 18 nm and 69%, respectively, in DNA solution (0.4 mg/mL) and AMD (25 μM) in 25 mM phosphate buffer at pH 7.02.[30]

The mean binding constants for AMD and N8AMD with the oligonucleotide species (Table 2) indicate that AMD molecules bind more strongly to the oligonucleotide than the N8AMD molecules do. This is quite consistent with the fact that the N8AMD molecule can form an additional hydrogen bond with a water molecule (N8···H-O-H) in aqueous solution, which the AMD molecule cannot form. Probably this hydrogen bonding stabilizes the N8AMD molecules in solution and tends to prevent intercalation of the N8AMD molecules into the nucleic acid. As a result, the binding constant of N8AMD is less than that of AMD. The other significant difference between AMD and N8AMD is the ratio of binding constants with DNA:DNA and RNA:DNA. The ratio of AMD–DNA:DNA and AMD–RNA:DNA is 79 ($(2.7 \times 10^6)/(3.4 \times 10^4) = 79$), whereas the corresponding ratio of N8AMD–DNA:DNA and N8AMD–RNA:DNA is 2.4 ($(3.9 \times 10^4)/(1.6 \times 10^4) = 2.4$). This large difference between the ratios indicates that the N8AMD molecule binds relatively more favorably to the RNA:DNA hybrid than the AMD molecule. Such a tendency toward RNA:DNA hybrid selectivity of N8AMD should be created by introducing the N8-atom in the chromophore. The N8-atom probably participates in an additional hydrogen bond (N8···H-O2′) with the 2′-hydroxyl group of RNA in the N8AMD–RNA:DNA complex, but such a hydrogen bond cannot be formed in the AMD–RNA:DNA complex.

Conclusion

N8AMD has been successfully synthesized by coupling the pyridine and benzene fragments. As predicted by molecular mechanics calculations and X-ray crystallographic studies, both AMD and N8AMD bind intercalatively not only to the DNA:DNA double strands but also to the RNA:DNA hybrids. Although the overall binding capacity of N8AMD is reduced substantially in comparison with that of AMD, N8AMD tends to bind relatively more favorably to the RNA:DNA hybrid. Thus, this initial attempt at designing an RNA:DNA hybrid binding agent appears to be successful. However, it is necessary to modify the agent further to increase its RNA:DNA hybrid binding character and to decrease the DNA:DNA binding character, in order to make a useful RNA:DNA hybrid binding agent.

Experimental Section

Molecular Modeling. The molecular mechanics calculations have been applied to investigation of the RNA:DNA–N8AMD interaction using the program AMBER version 4.0.[22] Visualization and model building were carried out using TOM/FRODO.[32] All of the calculations were performed on an IBM RISC-6000/550 workstation. Atomic charges and force field parameters for the nucleic acid portion of the system were taken from the standard AMBER distribution. Charges for the nonstandard amino acids (sarcosine and *N*-methylvaline), peptide lactone, and chromophores were calculated with the electrostatic potential (ESP)[33] enhancements of MOPAC 5.5[34] using AM1[35] optimized model tripeptides (Gly-Xxx-Gly) and a small phenoxazinone derivative. A single sodium ion was added to each phosphate group with AMBER's automatic routine of counterion generation, in order to balance charges. All calculations were done with a 9-Å cutoff criteria. Four models were individually refined by the molecular mechanics method to minimize the total energy of the system.

Syntheses. Melting points are uncorrected. The NMR spectra were obtained with 300-MHz Varian XL-300 NMR Spectrometer. For the mass spectrum measurements, electron ionization (EI) and chemical ionization (CI) spectra were obtained on a Nermag R10-10 quadrupole GC/MS system with SPECTRAL 30 data system. Fast-atom bombardment mass spectra (FABMS) were obtained on a ZAB HS mass spectrometer. All mass spectrum measurements have been carried out at the Mass Spectrometry Laboratory of the University of Kansas, under director T. D. Williams. The homogeneity of the products was checked by thin-layer chromatography on silica gel plates.

2,5-Dimethyl-4-nitropyridine 1-Oxide (1). To a solution of 2,5-dimethylpyridine (32.0 g, 0.30 mol) in acetic acid (120 mL) was added 29% H_2O_2 (21 mL) at 55 °C, and stirring was maintained for 12 h at this temperature before another 29% H_2O_2 (19 mL) was added. After stirring at 60 °C for 12 h, the solution was concentrated to 80 mL *in vacuo* and water (100 mL) was added. The mixture was further concentrated *in vacuo* to 50 mL, and solid Na_2CO_3 was added to the solution until no further evolution of CO_2 was observed. The reaction mixture was extracted with $CHCl_3$ (2 × 150 mL). The combined $CHCl_3$ extracts were washed with water (2 × 50 mL) and dried over Na_2SO_4, and evaporation of $CHCl_3$ gave 35.0 g of 2,5-dimethylpyridine 1-oxide as a colorless liquid. Without further purification, the 2,5-dimethylpyridine 1-oxide was slowly added to a stirred mixture of 90% HNO_3 (29 mL) and 98% H_2SO_4 (120 mL) over 30 min. The mixture was stirred at 90 °C for 4 h, poured onto ice (500 g), and neutralized with Na_2CO_3 to pH 7. The resulting precipitate was collected and recrystallized from ethanol to give 34.0 g (68%) of **1** as yellow needles: mp 149–150 °C [lit.[36] 152 °C]; NMR ($CDCl_3$) δ 2.53 (3H, s, Ar-CH_3), 2.59 (3H, s, Ar-CH_3), 8.03 (1H, s, Ar-H), 8.20 (1H, s, Ar-H).

4-Chloro-2,5-dimethylpyridine 1-Oxide (2). A solution of **1** (20.0 g, 0.119 mol) in cold acetyl chloride (0 °C, 100 mL) was heated to 55 °C for 0.5 h, then cooled to room temperature, poured into ice water (300 mL), and neutralized with Na_2CO_3 to pH 7. The aqueous solution was extracted with $CHCl_3$ (3 × 100 mL). The combined $CHCl_3$ extracts were washed with water (2 × 50 mL) and dried over Na_2SO_4. After evaporation of $CHCl_3$, the residue was recrystallized from hexane to give 14.6 g (78%) of **2** as colorless crystals: mp 90–91 °C; NMR ($CDCl_3$) δ 2.29 (3H, s, 5-CH_3), 2.48 (3H, s, 2-CH_3), 7.25 (1H, s, 3-H), 8.17 (1H, s, 6-H); EIMS *m/z* (relative intensity) 157 (M, 85); HRMS calcd for C_7H_8ClNO 157.0294, found 157.0301.

2,5-Dimethyl-4-methoxypyridine 1-Oxide (3). To a solution of sodium methoxide obtained from Na (11.5 g, 0.50 mol) and methanol (230 mL) was added **2** (15.6 g, 0.099 mol) at 25 °C. The mixture was heated at reflux for 3 h. After evaporation of the solution, the residue was dissolved in water (50 mL) and neutralized with HCl (1:1) to pH 7. The aqueous solution was extracted with $CHCl_3$ (3 × 70 mL). The combined $CHCl_3$ extracts were washed with water (2 × 50 mL) and dried over Na_2SO_4. After evaporation of $CHCl_3$, the residue was recrystallized from hexane to give 14.0 g (93%) of **3** as colorless needles: mp 84–85 °C; NMR ($CDCl_3$) δ 2.13 (3H, s, 5-CH_3), 2.53 (3H, s, 2-CH_3), 3.88 (3H, s, 4-OCH_3), 6.66 (1H, s, 3-H), 8.07 (1H, s, 6-H); EIMS *m/z* (relative intensity) 153 (M, 95); HRMS calcd for $C_8H_{11}NO_2$ 153.0790, found 153.0799.

2,5-Dimethyl-4-methoxypyridine (4). To a solution of **3** (8.4 g, 55 mmol) in $CHCl_3$ (120 mL) was added PCl_3 (16 mL) at 0 °C. The resulting mixture was kept at 25 °C for 1 h before it was heated to 80–85 °C for 0.5 h with stirring. After evaporation of $CHCl_3$, the residue was dissolved in water (80 mL) and neutralized with Na_2CO_3 to pH 7. The aqueous solution was extracted with $CHCl_3$ (3 × 70 mL). The combined $CHCl_3$ extracts were washed with water (2 × 50 mL) and dried over Na_2SO_4. Evaporation of $CHCl_3$ and distillation of the residue gave 7.1 g (94%) of **4** as colorless liquid: bp 54–55 °C at 1 mmHg; NMR ($CDCl_3$) δ 2.13 (3H, s, 2-CH_3), 2.51 (3H, s, 5-CH_3), 3.85 (3H, s, 4-OCH_3), 6.60 (1H, s, 3-H), 8.12 (1H, s, 6-H); EIMS *m/z* (relative intensity) 137 (M, 95); HRMS calcd for $C_8H_{11}NO$ 137.0841, found 137.0849.

2,5-Dimethyl-4-methoxy-3-nitropyridine (5). To a solution of **4** (10.5 g, 77 mmol) in 98% H_2SO_4 (200 mL) were added 90% HNO_3 (15 mL) and 98% H_2SO_4 (100 mL) at 5 °C. The resulting mixture was stirred and heated at 80–85 °C for 1 h. The reaction mixture was poured onto ice (700 g) and neutralized with Na_2CO_3 to pH 7. The aqueous solution was extracted with $CHCl_3$ (4 × 100 mL). The combined $CHCl_3$ extracts were washed with water (2 × 100 mL) and dried over Na_2SO_4. After evaporation of $CHCl_3$, the residue was recrystallized from hexane to give 8.5 g (61%) of **5** as pale yellow crystals: mp 36–37 °C; NMR ($CDCl_3$) δ 2.31 (3H, s, 5-CH_3), 2.51 (3H, s, 2-CH_3), 3.95 (3H, s, 4-OCH_3), 8.36 (1H, s, 6-H); EIMS *m/z* (relative intensity) 182 (M, 77); HRMS calcd for $C_8H_{10}N_2O_3$ 182.0691, found 182.0697.

2,5-Dimethyl-4-methoxy-3-nitropyridine 1-Oxide (6). To a solution of **5** (9.0 g, 49 mmol) in $CHCl_3$ (100 mL) was added 80–90% *m*-chloroperbenzoic acid (16.0 g) at 0 °C. The mixture was stirred at 25 °C for 36 h. The reaction mixture was washed with 10% Na_2CO_3 (3 × 100 mL) and water (2 × 100 mL) and dried over Na_2SO_4. After evaporation of $CHCl_3$, the residue was recrystallized from ethanol to give 9.6 g (98%) of **6** as yellow crystals: mp 107–109 °C; NMR ($CDCl_3$) δ

(32) Jones, T. A.; Thirup, S. *EMBO J.* **1986**, *5*, 819–822.
(33) Besler, B. H.; Merz, K. M., Jr.; Kollman, P. A. *J. Comput. Chem.* **1990**, *11*, 431–439.
(34) Stewart, J. J. P. *MOPAC*, QCPE #455, Version 5.0, 1985.
(35) Dewar, M. J. S.; Zoebisch, E. G.; Healy, E. F.; Stewart, J. J. P. *J. Am. Chem. Soc.* **1985**, *107*, 3902–3909.
(36) Koncewicz, J.; Skrowazewska, Z. *Rocz. Chem.* **1968**, *42*, 1873–1885.

2.31 (3H, s, 5-CH_3), 2.46 (3H, s, 2-CH_3), 3.93 (3H, s, 4-OCH_3), 8.23 (1H, s, 6-H); CIMS *m/z* (relative intensity) 199 (M + H, 98); HRMS calcd for $C_8H_{10}N_2O_4$ 198.0641, found 198.0632.

4-Methoxy-5-methyl-3-nitro-2-pyridinemethanol Acetate (7). A solution of **6** (9.6 g, 48 mmol) in acetic anhydride (50 mL) was stirred and heated to 120–122 °C for 3 h. After evaporation of the solution, the residue was distilled *in vacuo* to give 7.1 g (61%) of **7** as mobile orange liquid: bp 125–134 °C at 1 mmHg; NMR ($CDCl_3$) δ 2.10 (3H, s, –$OCOCH_3$), 2.36 (3H, s, 5-CH_3), 3.97 (3H, s, 4-OCH_3), 5.24 (2H, s, 2-CH_2OH), 8.47 (1H, s, 6-H); CIMS *m/z* (relative intensity) 241 (M + 1, 12); HRMS calcd for $C_{10}H_{13}N_2O_5$ (M + H) 241.0824, found 241.0827.

4-Methoxy-5-methyl-3-nitro-2-pyridinemethanol (8). After hydrolysis of **7** (2.00 g, 8.0 mmol) with 8% KOH (20 mL) at 25 °C for 24 h, the solution was neutralized with HCl (1:1) to pH 7. The reaction mixture was extracted with $CHCl_3$ (3 × 30 mL). The combined $CHCl_3$ extracts were washed with water (2 × 30 mL) and dried over Na_2SO_4. After evaporation of $CHCl_3$, the residue was recrystallized from hexane–ethyl acetate (2:1) to give 0.85 g (52%) of **8** as pale yellow crystals: mp 49–50 °C; NMR ($CDCl_3$) δ 2.33 (3H, s, 5-CH_3), 3.96 (3H, s, 4-OCH_3), 4.72 (2H, s, 2-CH_2OH), 8.44 (1H, s, 6-H); CIMS *m/z* (relative intensity) 199 (M + H, 26); HRMS calcd for $C_8H_9N_2O_4$ (M – H) 197.0562, found 197.0562.

4-Methoxy-5-methyl-3-nitro-2-pyridinecarboxylic Acid (9). A solution of **8** (1.22 g, 6.0 mmol) in 10% Na_2CO_3 (7.8 mL) was oxidized with 1.22 g of $KMnO_4$ in water (32 mL) at 25 °C for 4 h with stirring. After elimination of solid MnO_2, the solution was neutralized with HCl (1:1) to pH 4. The resulting precipitate was collected and recrystallized from ethanol to give 1.07 g (82%) of **9** as colorless needles: mp 128 °C (dec); NMR (DMSO-d_6) δ 2.41 (3H, s, 5-CH_3), 3.94 (3H, s, 4-OCH_3), 8.66 (1H, s, 6-H); CIMS *m/z* (relative intensity) 213 (M + H, 70); HRMS calcd for $C_8H_9N_2O_5$ (M + H) 213.0511, found 213.0533.

1,4-Dihydro-5-methyl-3-nitro-4-oxo-2-pyridinecarboxylic Acid (10). A solution of **9** (1.45 g, 6.8 mmol) in 48% HBr (15 mL) was stirred and heated at 80–82 °C for 4 h. After evaporation of the solution, the residue was washed with water (5 mL) to give 1.30 g (96%) of **10** as a white amorphous powder: mp >300 °C; NMR (DMSO-d_6) δ 1.98 (3H, s, 5-CH_3), 7.78 (1H, s, 6-H); EIMS *m/z* (relative intensity) 198 (M, 20); HRMS calcd for $C_7H_7N_2O_5$ (M + H) 199.0355, found 199.0333.

Methyl 1,4-Dihydro-5-methyl-3-nitro-4-oxo-2-pyridinecarboxylate (11). A solution of **10** (1.30 g, 6.57 mmol) in methanol (13 mL) was refluxed 12 h under bubbling dry HCl gas. The reaction mixture was kept at 5 °C for 2 h, and the resulting precipitate was collected and recrystallized from ethanol to give 0.86 g (62%) of **11** as colorless needles: mp 240–241 °C; NMR (DMSO-d_6) δ 2.00 (3H, s, 5-CH_3), 3.90 (3H, s, –$COOCH_3$), 7.84 (1H, s, 6-H); EIMS *m/z* (relative intensity) 212 (M, 50), 180 (90), 108 (90); CIMS in NH_3 *m/z* (relative intensity) 213 (M + 1, 90); HRMS calcd for $C_8H_9N_2O_5$ (M + H) 213.0511, found 213.0536.

Methyl 1,4-Dihydro-3-amino-5-methyl-4-oxo-2-pyridinecarboxylate (12). A solution of **11** (250 mg, 1.18 mmol) in methanol (20 mL) was hydrogenated over 5% Pd/C (130 mg) at atmospheric pressure for 2 h with stirring. After filtration, the filtrate was evaporated and the residue was recrystallized from ethanol to give 205 mg (96%) of **12** as colorless crystals: mp 192–193 °C; NMR (DMSO-d_6) δ 1.92 (3H, s, 5-CH_3), 3.88 (3H, s, –$COOCH_3$), 6.18 (2H, s, 3-NH_2), 7.38 (1H, s, 6-H); EIMS *m/z* (relative intensity) 182 (M, 70); HRMS calcd for $C_8H_{10}N_2O_3$ 182.0691, found 182.0686.

Methyl 2-Amino-3-hydroxy-4-methylbenzoate Hydrochloride (13). A solution of 3-hydroxy-4-methyl-2-nitrobenzoic acid (3.72 g, 18.9 mmol) in methanol (20 mL) was refluxed under bubbling dry HCl gas for 10 h. After evaporation of the solution, the residue was recrystallized from ethanol to give 2.70 g (68%) of methyl 3-hydroxy-4-methyl-2-nitrobenzoate as colorless needles: mp 115–117 °C. A solution of the product (372 mg, 1.76 mmol) in methanol (20 mL) was hydrogenated over 5% Pd/C (185 mg) at atmospheric pressure for 2 h with stirring. After filtration, the filtrate was evaporated and a solution of the residue in ether (30 mL) was bubbled by dry HCl gas for 5 min. The resulting precipitate was collected to afford 300 mg (78%) of **13** as colorless needles: mp 162–163 °C (lit.[37] 168–170 °C).

Dimethyl 2-Amino-4,6-dimethyl-3-oxo-8-azaphenoxazine-1,9-dicarboxylate (14a). A solution of **12** (100 mg, 0.54 mmol) in methanol (5 mL) was added to a stirred solution of $K_3Fe(CN)_6$ (87 mg, 0.27 mmol) in 200-mmol acetate buffer (pH 4.75, 25 mL) at 25 °C. Solutions of **13** (60 mg, 0.27 mmol) in 200-mmol acetate buffer (pH 4.75, 25 mL) and $K_3Fe(CN)_6$ (174 mg, 0.54 mmol) in water (10 mL) were independently but simultaneously added drop by drop into a stirred solution of **12** in 15 min at 25 °C. After the mixture was stirred at 25 °C for 15 min, the resulting precipitate was collected and recrystallized from pyridine to give 50 mg (51%) of **14a** as red needles: mp 241–243 °C (dec); NMR ($CDCl_3$) δ 2.23 (3H, s, 4-CH_3), 2.50 (3H, s, 6-CH_3), 4.00 (3H, s, 1-$COOCH_3$), 4.06 (3H, s, 9-$COOCH_3$), 8.43 (1H, s, 7-H); EIMS *m/z* (relative intensity) 357 (M, 55); CIMS *m/z* (relative intensity) 358 (M + H, 90); HRMS calcd for $C_{17}H_{15}N_3O_6$ 357.0961, found 357.0935.

Dimethyl 2-Amino-4,6-dimethyl-3-oxophenoxazine-1,9-dicarboxylate (14b). A solution of methyl 3-hydroxy-4-methyl-2-nitrobenzoate (100 mg, 0.47 mmol) in methanol (10 mL) was hydrogenated over 10% Pd/C (50 mg) for 2 h at atmospheric pressure. After filtration of the catalyst, the filtrate was added to a solution of $K_3Fe(CN)_6$ (465 mg, 1.41 mmol) in 67-mmol phosphate buffer (pH 7.12, 15 mL) at 40 °C. The mixture was stirred at 40 °C for 20 min, extracted with $CHCl_3$ (25 mL × 3), washed with water (20 mL), and dried over Na_2SO_4, and evaporation of $CHCl_3$ gave a orange solid. Recrystallization from ethyl acetate gave 56 mg (67%) of **14b** as an orange needled crystal: mp 194–195 °C (dec) (lit.[37] 195–198 °C); NMR ($CDCl_3$) δ 2.23 (3H, s, 4-CH_3), 2.53 (3H, s, 6-CH_3), 4.00 (3H, s, $COOCH_3$), 4.01 (3H, s, $COOCH_3$), 7.31 (1H, d, 7-H), 7.62 (1H, d, 8-H); CIMS *m/z* (relative intensity) 357 (M + 1, 91); indicated M = 356 ($C_{18}H_{16}N_2O_6$ requires M = 356.33).

***N*-(Benzyloxycarbonyl)prolylsarcosine *tert*-Butyl Ester (15).** A solution of (benzyloxycarbonyl)sarcosine *tert*-butyl ester (4.82 g, 17.3 mmol) in methanol (30 mL) was hydrogenated over 10% Pd/C (560 mg) at atmospheric pressure for 2 h with stirring. After filtration, the filtrate was evaporated *in vacuo*. To a solution of the residue and (benzyloxycarbonyl)proline (4.3 g, 17.3 mmol) in dichloromethane (40 mL) was added a solution of DCC (3.56 g, 17.3 mmol) in dichloromethane (10 mL) at –10 °C. The reaction mixture was stirred 3 h at –10 °C and then kept overnight in a refrigerator. After removal of *N,N'*-dicyclohexylurea (DCurea) by filtration, the filtrate was evaporated *in vacuo*. The residue was dissolved in ethyl acetate (80 mL), and the solution was washed with 10% citric acid (2 × 15 mL), 1 M $NaHCO_3$ (2 × 15 mL), and water (20 mL) and dried over Na_2SO_4. After evaporation of the ethyl acetate *in vacuo*, the residue was subjected to flash chromatography on silica gel with ethyl acetate–hexane (1:2) to afford 5.65 g (87%) of **15** as a colorless liquid: $[\alpha]^{23}_D$ –57.4° (*c* 1.0, CH_3OH) [lit.[25] $[\alpha]^{20}_D$ –58.0° (*c* 1.0, CH_3OH)]; NMR ($CDCl_3$) δ 7.33 (5H, m, BzlAr-H), 5.08 (2H, s, Ar-CH_2), 3.12 (3H, s, NCH_3), 1.45 (9H, s, OtBu).

***N*-(Benzyloxycarbonyl)-D-valylprolylsarcosine *tert*-Butyl Ester (16).** A solution of **15** (2.70 g, 7.2 mmol) in methanol (25 mL) was hydrogenated over 10% Pd/C (350 mg) at atmospheric pressure for 2 h with stirring. After filtration the filtrate was evaporated *in vacuo*. A solution of the residue and (benzyloxycarbonyl)-D-valine (1.80 g, 7.2 mmol) in dichloromethane (25 mL) was added to a solution of DCC (1.50 g, 7.2 mmol) in dichloromethane (5 mL) at –10 °C. The reaction mixture was stirred 3 h at –10 °C and then kept overnight in a refrigerator. After removal of DCurea by filtration, the filtrate was evaporated *in vacuo*. The residue was dissolved in ethyl acetate (75 mL), and the solution was washed with 10% citric acid (2 × 10 mL), 1 M $NaHCO_3$ (2 × 10 mL), and water (2 × 15 mL) and dried over Na_2SO_4. After evaporation of the ethyl acetate *in vacuo*, the residue was subjected to flash chromatography on silica gel with ethyl acetate–hexane (1:1) to afford 2.76 g (81%) of **16** as a colorless liquid: $[\alpha]^{23}_D$ –33.1° (*c* 1.1, CH_3OH), [lit.[25] $[\alpha]^{20}_D$ –33.5° (*c* 1.0, CH_3OH)]; NMR ($CDCl_3$) δ 7.34 (5H, s, BzlAr-H), 5.10 (2H, s, Ar-CH_2), 3.13 (3H, s, N-CH_3), 1.45 (9H, s, OtBu), 0.98 (3H, d, Val-CH_3), 0.89 (3H, d, Val-CH_3); CIMS *m/z* (relative intensity) 476 (M + 1, 4).

***N*-(Benzyloxycarbonyl)threonyl-D-valylprolylsarcosine *tert*-Butyl Ester (17).** A solution of **16** (2.60 g, 5.47 mmol) in methanol (25 mL) was hydrogenated over 10% Pd/C (300 mg) at atmospheric pressure for 2 h with stirring. After filtration the filtrate was evaporated *in vacuo*. To a solution of the residue and (benzyloxycarbonyl)threonine (1.38 g, 5.45 mmol) in dichloromethane (20 mL) was added a solution of DCC (1.13 g, 5.47 mmol) in dichloromethane (5 mL) at –10 °C. The reaction mixture was stirred 3 h at –10 °C and then kept overnight in a refrigerator. After removal of DCurea by filtration, the filtrate was evaporated *in vacuo*. The residue was dissolved in ethyl acetate (80 mL), and the solution was washed with 10% citric acid (2 × 20 mL), 1 M $NaHCO_3$ (2 × 15 mL), and water (2 × 20 mL) and dried over Na_2SO_4. After evaporation of the ethyl acetate *in vacuo*, the residue was subjected to flash chromatography on silica gel with ethyl acetate to afford 2.15 g (69%) of **17** as a white amorphous solid: $[\alpha]^{23}_D$ –39.7° (*c* 1.0, CH_3OH); NMR ($CDCl_3$) δ 7.33 (5H, s, BzlAr-H), 5.12 (2H, s, Ar-CH_2), 3.07 (3H, s, NCH_3), 1.42 (9H, s, OtBu), 1.20 (3H, d, Thr-CH_3), 0.88 (3H, d, Val-CH_3), 0.80 (3H, d, Val-CH_3); CIMS *m/z* (relative intensity) 577 (M + H, 74); HRMS calcd for $C_{29}H_{45}N_4O_8$ (M + H) 577.3237, found 577.3256.

***O*-(*tert*-Butoxycarbonyl)-*N*-methylvalyl-*N*-(benzloxycarbonyl)-**

(37) Angyal, S. J.; Bullock, E.; Hanger, W. G.; Howell, W. C.; Johnson, A. W. *J. Chem. Soc.* **1957**, 1592–1602.

threonyl-D-valylprolylsarcosine *tert*-Butyl Ester (18). To a solution of **17** (1.33 g, 2.31 mmol) and (*tert*-butoxycarbonyl)-*N*-methylvaline (0.64 g, 2.77 mmol) in dichloromethane (15 mL) were added *N,N*-(dimethylamino)pyridine (140 mg, 1.15 mmol) and a solution of DCC (570 mg, 2.77 mmol) in dichloromethane (10 mL) at 0 °C. The reaction mixture was stirred for 2 h at 0 °C and 12 h at room temperature. After removal of DCurea by filtration, the filtrate was evaporated *in vacuo*. The residue was dissolved in ethyl acetate (80 mL), and the solution was washed with 10% citric acid (2 × 15 mL), 1 M $NaHCO_3$ (2 × 15 mL), and water (2 × 20 mL) and dried over Na_2SO_4. After evaporation of the ethyl acetate *in vacuo*, the residue was subjected to flash chromatography on silica gel with ethyl acetate–hexane (2:1) to afford 1.49 g (82%) of **18** as a white amorphous solid: $[\alpha]^{23}_D$ −36.6° (*c* 1.0, CH_3OH); NMR ($CDCl_3$) δ 7.34 (5H, s, BzylAr-H), 5.11 (2H, s, Ar-CH_2), 3.11 (3H, s, NCH_3), 2.78 (3H, s, NCH_3), 1.43 (18H, s, OtBu), 1.23 (3H, d, Thr-CH_3), 0.91 (6H, d, MeVal-CH_3), 0.85 (6H, d, Val-CH_3); CIMS in NH_3 *m/z* (relative intensity) 790 (M + H, 2); HRMS calcd for $C_{40}H_{64}N_5O_{11}$ (M + H) 790.4602, found 790.4638.

***N*-(Benzyloxycarbonyl)threonyl-D-valylprolylsarcosyl-*N*-methylvaline Lactone (19).** A solution of **18** (0.64 g, 0.81 mmol) in trifluoroacetic acid (7 mL) was stirred at 0 °C for 4 h. After evaporation of the trifluoroacetic acid *in vacuo*, the residue was dissolved in ethyl acetate (60 mL) and then evaporated *in vacuo*. To the residue was added ethyl ether (80 mL), and the solid was filtered to give a deprotected peptide salt with trifluoroacetic acid. To a solution of the solid in dichloromethane (100 mL) was added triethylamine (174 mg, 1.73 mmol) at 0 °C, and the mixture was diluted with dichloromethane (400 mL) and *N,N*-bis(2-oxo-3-oxazolidinyl)phosphorodiamidic chloride (293 mg, 1.15 mmol) was added. The reaction mixture was stirred for 5 days at 23 °C. After evaporation of the solution, the residue was dissolved in ethyl acetate (50 mL) and the solid was filtered off. The filtrate was evaporated, and the residue was subjected to flash chromatography on silica gel with ethyl acetate–methanol (10:1) to afford 295 mg (59%) of **19** as a white amorphous solid: $[\alpha]^{23}_D$ −31.6° (*c* 0.6, CH_3OH); NMR (CD_3COCD_3) δ 7.90 (1H, d, Thr-NH), 7.39 (5H, s, Ar-H), 6.02 (1H, d, Val-NH), 5.09 (2H, d, Ar-CH_2), 3.24 (3H, s, MeVal-NCH_3), 2.86 (3H, s, Sar-NCH_3, 1.21 (3H, d, Thr-CH_3), 1.05 (3H, d, Val-CH_3), 1.02 (3H, d, Val-CH_3, 0.86 (3H, d, MeVal-CH_3), 0.82 (3H, d, MeVal-CH_3); CIMS in NH_3 *m/z* (relative intensity) 616 (M + H, 41); HRMS calcd for $C_{31}H_{44}N_5O_8$ (M + H) 616.3346, found 616.3337.

(5-Methyl-4-methoxy-3-nitro-2-pyridinoyl)threonyl-D-valylprolylsarcosyl-*N*-methylvaline Lactone (20). A solution of **19** (1.86 g, 3.02 mmol) in methanol (30 mL) was hydrogenated over 10% Pd/C (250 mg) at atmospheric pressure for 2 h at room temperature. After the catalyst was filtered off, the filtrate was evaporated and the residue was dissolved in CH_2Cl_2 (40 mL) and **9** (0.77 g, 3.63 mmol) was added. Then a solution of DCC (0.76 g, 3.63 mmol) was added to the mixture at −10 °C. The mixture was kept at −10 °C for 3 h and overnight in a refrigerator. After removal of DCurea by filtration, the filtrate was dissolved in ethyl acetate (85 mL), washed with 1 M $NaHCO_3$ (25 mL × 2) and water (30 mL), and dried over Na_2SO_4. After evaporation of the solvent, the residue was purified by flash chromatography (EtOAc–MeOH) to afford 1.42 g (71%) of **20** as a colorless solid: $[\alpha]^{23}_D$ −18.8° (*c* 1.0, CH_3OH); NMR (CD_3COCD_3) δ 8.65 (1H, s, Ar-6H), 8.56 (1H, d, Thr-NH), 4.01 (3H, s, Ar-OCH_3), 3.33 (3H, s, MeVal-NCH_3), 2.88 (3H, s, Sar-NCH_3), 2.50 (3H, s, ArCH_3), 1.20 (3H, s, Thr-CH_3), 1.05 (3H, d, Val-CH_3), 1.02 (3H, d, Val-CH_3), 0.87 (3H, d, MeVal-CH_3), 0.81 (3H, d, MeVal-CH_3); CIMS in NH_3 *m/z* (relative intensity) 676 (M + H, 60); HRMS calcd for $C_{31}H_{46}N_7O_{10}$ (M + H) 676.3306, found 676.3325.

(1,4-Dihydro-5-methyl-3-nitro-4-oxo-2-pyridinoyl)threonyl-D-valylprolylsarcosyl-*N*-methylvaline Lactone (21). To a solution of **20** (68 mg, 0.10 mmol) in CH_2Cl_2 (2 mL) was added 1 M BBr_3 in CH_2Cl_2 (0.15 mL, 0.15 mmol) at room temperature. The mixture was stirred at room temperature for 16 h. After evaporation of the solvent, the residue was dissolved in ethyl acetate (10 mL). Two drops of water were added, the solvent was evaporated, and the residue was purified by flash chromatography (EtOAc/MeOH (10:3)) to afford 55 mg (83%) of **21** as a yellow solid: $[\alpha]^{23}_D$ −25.1° (*c* 0.9, CH_3OH); NMR (CD_3COCD_3) δ 9.10 (1H, d, Thr-NH), 7.46 (1H, s, Ar-6H), 3.25 (3H, s, MeVal-NCH_3), 2.86 (3H, s, Sar-NCH_3), 1.97 (3H, s, Ar-CH_3), 1.38 (3H, d, Thr-CH_3), 1.11 (3H, d, Val-CH_3), 1.03 (3H, d, Val-CH_3), 0.99 (3H, d, MeVal-CH_3), 0.88 (3H, d, MeVal-CH_3); FABMS 662 (M + H, 100), 684 (M + Na, 35); HRMS calcd for $C_{30}H_{44}N_7O_{10}$ (M + H) 662.3150, found 662.3142.

(1,4-Dihydro-5-methyl-3-amino-4-oxo-2-pyridinoyl)threonyl-D-valylpropylsarcosyl-*N*-methylvaline Lactone (22). A solution of **21** (55 mg, 0.083 mmol) in methanol (10 mL) was hydrogenated over 10% Pd/C (15 mg) at atmospheric pressure for 2 h. After the catalyst was filtered off, the filtrate was evaporated and the residue was purified by flash chromatography (EtOAc–MeOH (10:2)) to afford 43 mg (83%) of **22** as a colorless solid: $[\alpha]^{23}_D$ −11.0° (*c* 0.6, CH_3OH); NMR (CD_3COCD_3) δ 7.61 (1H, s, Ar-6H), 3.33 (3H, s, MeVal-NCH_3), 2.89 (3H, s, Sar-NCH_3), 1.97 (3H, s, Ar-5-CH_3), 1.28 (3H, d, Thr-CH_3), 1.07 (3H, d, Val-CH_3), 1.02 (3H, d, Val-CH_3), 0.90 (3H, d, MeVal-CH_3), 0.84 (3H, d, MeVal-CH_3); FABMS (relative intensity) 632 (M + H, 100), 654 (M + Na, 8); HRMS calcd for $C_{30}H_{46}N_7O_8$ (M + H) 632.3408, found 632.3427.

(3-(Benzyloxy)-4-methyl-2-nitrobenzoyl)threonyl-D-valylprolylsarcosyl-*N*-methylvaline Lactone (23). A solution of **19** (1.00 g, 1.63 mmol) in methanol (15 mL) was hydrogenated over 10% Pd/C (0.15 g) at atmospheric pressure for 2 h. After the catalyst was filtered off, the filtrate was evaporated *in vacuo* and the residue was dissolved in CH_2Cl_2 (15 mL). Then 3-(benzyloxy)-4-methyl-2-nitrobenzoic acid (513 mg, 1.79 mmol) was added. To the mixture was added a solution of DCC (376 mg, 1.79 mmol) in CH_2Cl_2 (5 mL) at 0 °C. The mixture was kept at 0 °C for 3 h and overnight at room temperature. After removal of DCurea by filtration, the filtrate was evaporated in vacuo and the residue was purified by flash chromatography (EtOAc–CH_2Cl_2–MeOH (10:10:1)) to afford 1.01 g (82%) of **23** as a colorless solid: $[\alpha]^{23}_D$ −10.5° (*c* 1.0, CH_3OH); NMR (CD_3COCD_3) δ 8.10 (1H, d, Thr-NH), 7.46–7.35 (7H, m, Ar-H), 5.05 (2H, s, Ar-CH_2), 3.32 (3H, s, MeVal-NCH_3), 2.88 (3H, s, Sar-NCH_3), 2.45 (3H, s, Ar-4-CH_3), 1.21 (3H, d, Thr-CH_3), 1.08 (3H, d, Val-CH_3), 1.02 (3H, d, Val-CH_3), 0.86 (3H, d, MeVal-CH_3), 0.84 (3H, d, MeVal-CH_3); CIMS (relative intensity) 751 (M + H, 50); HRMS calcd for $C_{38}H_{51}N_6O_{10}$ (M + H) 751.3667, found 751.3640.

N8-Actinomycin D (24a). A solution of **23** (60 mg, 0.08 mmol) in methanol (10 mL) was hydrogenated over Pd/C (15 mg) for 2 h. After the catalyst was filtered off, the filtrate and a solution of $K_3Fe(CN)_6$ (34 mg, 0.103 mmol) in 70 mM acetate buffer (pH 4.75, 5 mL) were added separately and drop by drop to a solution of **22** (43 mg, 0.068 mmol) in a mixture of MeOH (10 mL) and 70 mM acetate buffer (pH 4.75, 20 mL) including $K_3Fe(CN)_6$ (33 mg, 0.1 mmol). The mixture was stirred for 30 min at room temperature, water (25 mL) was added, and the mixture was extracted with EtOAc (2 × 30 mL). The extracts were washed with water (20 mL) and dried over Na_2SO_4. After evaporation of the solvent, the residue was purified by flash chromatography (EtOAc/MeOH (10:3)) to afford 45 mg (52%) of **24** as a red solid: $[\alpha]^{23}_D$ −235.0° (*c* 0.2, CH_3OH); NMR (CD_3COCD_3) δ 8.47 (1H, s, Ar-7H), 8.38 (1H, d, Thr-NH), 8.21 (1H, d, Thr-NH), 3.00 (6H, s, NCH_3), 2.98 (6H, s, NCH_3), 2.53 (3H, s, Ar-6CH_3), 2.17 (3H, s, Ar-4CH_3), 1.30 (6H, d, Thr-CH_3), 0.98 (6H, d, Val-CH_3), 0.90 (6H, d, Val-CH_3), 0.87 (6H, d, MeVal-CH_3), 0.79 (6H, d, MeVal-CH_3); FABMS 1257 (M + H, 21), 1279 (M + Na, 5); HRMS calcd for $C_{61}H_{86}N_{13}O_{16}$ (M + H) 1256.6316, found 1256.6361.

Actinomycin D (24b). A solution of **23** (0.100 g, 0.12 mmol) in methanol (15 mL) was hydrogenated over 10% Pd/C (40 mg) at atmospheric pressure for 2 h with stirring. After filtration, the filtrate was added a solution of 67 mM phosphate buffer, pH 7.1 (20 mL), containing potassium hexacyanoferrate(III) (0.118 g, 0.36 mmol). The mixture was stirred for 10 min at room temperature, and then water (50 mL) was added and the solution extracted with ethyl acetate (3 × 30 mL). The extracts were washed with water (20 mL) and dried over Na_2SO_4. After evaporation of the ethyl acetate, the residue was recrystallized from ethyl acetate to afford 50 mg (59%) of **22** as a red amorphous solid: $[\alpha]^{23}_D$ −335.0° (*c* 0.2, CH_3OH); NMR (CD_3COCD_3) δ 8.24 (1H, d, NH), 8.18 (1H, d, NH), 7.79 (1H, d, NH), 7.45 (1H, d, NH), 7.61 (1H, d, 8-H), 7.49 (1H, d, 7-H), 2.97 (3H, s, NCH_3), 2.93 (3H, s, NCH_3), 2.83 (3H, s, NCH_3), 2.82 (3H, s, NCH_3), 2.58 (3H, s, 6-CH_3), 2.16 (3H, s, 4-CH_3), 1.27 (3H, d, Thr-CH_3), 1.25 (3H, d, Thr-CH_3), 1.14 (3H, d, Val-CH_3), 1.12 (3H, d, Val-CH_3), 0.96 (6H, d, Val-CH_3), 0.87 (6H, d, MeVal-CH_3), 0.76 (6H, d, MeVal-CH_3); FABMS 1256 (M + H, 100), 1278 (M + Na, 14); HRMS calcd for $C_{62}H_{87}N_{12}O_{16}$ (M + H) 1255.6363, found 1255.6389.

X-ray Crystallography. All measurements were on a Rigaku AFC5R diffractometer with graphite-monochromated CuKα radiation (λ = 1.5418 Å) at 23 ± 2 °C and a 12-kW rotating anode generator. Cell constants and the orientation matrix for data collections were obtained from a least-squares refinement using the setting angles of 25 carefully centered reflections in the range of $60.0° < 2\theta < 70.0°$. The data were collected using the ω–2θ scan technique to a maximum 2θ value of 112.5°. ω scans of several intense reflections, made prior to data collection, had an average width at half-height of 0.45~0.51° with a take-off angle of 6.0°. Scans of $(1.73 + 0.30 \tan\theta)°$ were made at a speed of 32.0 deg/min (in ω). The weak reflections ($I < 10.0\sigma(I)$) were rescanned (maximum of three rescans), and the counts were accumulated to ensure good counting statistics. Stationary background counts were recorded on each side of

the reflection. The ratio of peak counting time to background counting time was 2:1. The diameter of the incident beam collimator was 0.5 mm, and the crystal to detector distance was 285.0 mm. The intensities of three representative reflections that were measured after every 150 reflections remained constant throughout data collection, indicating crystal and electronic stability (no decay correction was applied). Empirical absorption corrections, based on azimuthal scans of several reflections, were applied on all data. The data were corrected for Lorentz and polarization effects. The structures were solved by the direct method. The weighting scheme, w, was based on counting statistics and included a factor ($p = 0.05$) to down-weigh the intense reflections. The non-hydrogen atoms were refined anisotropically. The structures were refined by the full-matrix least-squares method minimizing $\sum w(|F_o| - |F_c|)^2$. The unweighted and weighted agreement factors are defined as $R = \sum||F_o| - |F_c||/\sum|F_o|$ and $R_w = [\sum w(|F_o| - |F_c|)^2/\sum wF_o^2]^{1/2}$, respectively. Neutral-atom scattering factors were taken from the *International Tables of X-ray Crystallography* (1974).[38] All calculations were performed using KUDNA[39] and TEXSAN[40] crystallographic software packages.

Crystal Structure Analysis of 12. A colorless prism crystal of $C_8H_{10}N_2O_3 \cdot H_2O$ having approximate dimensions of 0.80 × 0.50 × 0.30 mm was mounted on a glass fiber with epoxy glue. The crystal belongs to a monoclinic system of $a = 5.5194(8)$ Å, $b = 10.891(1)$ Å, $c = 15.930(2)$ Å, $\beta = 91.27(1)°$. On the basis of systematic absences of $h0l$, $h + l = 2n + 1$, and $0k0$, $k = 2n + 1$, and the successful solution and refinement of the structure, the space group was determined to be $P2_1/n$ (No. 14) and $Z = 4$. Of the 1498 reflections that were collected, 1336 were unique ($R_{int} = 0.033$). The final cycle of full-matrix least-squares refinement was based on 1141 observed reflections ($I > 3.00\sigma(I)$) and 175 variable parameters and converged (largest parameter shift was 0.03 times its esd) with $R = 0.077$ and $R_w = 0.089$. All hydrogen atoms were refined with isotropic thermal parameters. The maximum and minimum peaks on the final difference Fourier map corresponded to 0.29 and –0.22 e/Å^3, respectively.

Crystal Structure Analysis of 14a. A brawn plate crystal of $C_{17}H_{15}N_3O_6$ having approximate dimensions of 0.70 × 0.30 × 0.10 mm was mounted on a glass fiber with epoxy glue. The crystal belongs to a monoclinic system of $a = 7.764(1)$ Å, $b = 11.088(2)$ Å, $c = 9.660(2)$ Å, $\beta = 100.82(1)°$. On the basis of systematic absences of $h0l$, $l = 2n + 1$, and the successful solution and refinement of the structure, the space group was determined to be Pc (No. 7) and $Z = 2$. Of the 1239 reflections that were collected, 1144 were unique ($R_{int} = 0.058$). The final cycle of full-matrix least-squares refinement was based on 1039 observed reflections ($I > 3.00\sigma(I)$) and 257 variable parameters and converged (largest parameter shift was 0.13 times its esd) with unweighted and weighted agreement factors of $R = 0.046$ and $R_w = 0.057$. All hydrogen atoms were refined with isotropic thermal parameters. The maximum and minimum peaks on the final difference Fourier map corresponded to 0.13 and –0.12 e/Å^3, respectively.

Crystal Structure Analysis of 20. A colorless plate crystal of $C_{31}H_{45}N_7O_{10} \cdot \frac{1}{2}H_2O \cdot C_4H_8O_2$ having approximate dimensions of 0.50 × 0.30 × 0.10 mm was mounted on a glass fiber with epoxy glue. The crystal belongs to a monoclinic system of $a = 31.397(3)$ Å, $b = 13.927(2)$ Å, $c = 19.281(2)$ Å, $\beta = 99.51(1)°$. On the basis of systematic absences of hkl, $h + k = 2n + 1$, and the successful solution and refinement of the structure, the space group was determined to be $C2$ (No. 5) and $Z = 8$ (two molecules in an asymmetric unit). Of the 5897 reflections that were collected, 5769 were unique ($R_{int} = 0.036$). The final cycle of full-matrix least-squares refinement was based on 3113 observed reflections ($I > 3.00\sigma(I)$) and 893 variable parameters and converged (largest parameter shift was 0.35 times its esd) with unweighted and weighted agreement factors of $R = 0.071$ and $R_w = 0.087$. All hydrogen atoms were put in idealized positions with the same temperature parameters as those of attached non-hydrogen atoms. Heavily disordered solvents (ethyl acetate) were found, and no reasonable disordered model was made. Thus, the carbon atoms were put on the significant peak positions in the difference maps, and the occupancy parameters of the atoms were varied while the positional and thermal parameters ($B = 10.0$ Å^2) were fixed. The maximum and minimum peaks on the final difference Fourier map corresponded to 0.31 and –0.23 e/Å^3, respectively.

Crystal Structure Analysis of 19′. A colorless plate crystal of $C_{31}H_{45}N_5O_8 \cdot \frac{1}{2}H_2O \cdot \frac{1}{2}C_4H_8O_2$ having approximate dimensions of 0.50 × 0.30 × 0.10 mm was mounted on a glass fiber with epoxy glue. The crystal belongs to a monoclinic system of $a = 26.899(3)$ Å, $b = 11.623(2)$ Å, $c = 12.757(2)$ Å, $\beta = 110.15(1)°$. On the basis of systematic absences of hkl, $h + k = 2n + 1$, and the successful solution and refinement of the structure, the space group was determined to be $C2$ (No. 5) and $Z = 4$. Of the 2703 reflections that were collected, 2637 were unique ($R_{int} = 0.048$). The final cycle of full-matrix least-squares refinement was based on 1884 observed reflections ($I > 3.00\sigma(I)$) and 433 variable parameters and converged (largest parameter shift was 0.35 times its esd) with unweighted and weighted agreement factors of $R = 0.072$ and $R_w = 0.089$. All hydrogen atoms were put idealized positions with the same temperature parameters as those of attached non-hydrogen atoms. The solvent (ethyl acetate) was found to be 2-fold disordered and was included in refinement. The maximum and minimum peaks on the final difference Fourier map corresponded to 0.29 and –0.39 e/Å^3, respectively.

Binding Tests. UV/vis absorption spectra were measured on a JASCO V-560 double beam spectrometer. Each 15 μM scale of oligonucleotides (GGAGCAGGAC) and d(GTCCTGCTCC) and 2 μM r(GUCCUGCUCC) were synthesized by a Cruachem PS250 DNA/RNA synthesizer using the protocol provided from the company. After the deprotection procedure, the crude nucleotides were purified by a reverse phase HPLC using the C_{18} columns. DNA and RNA solutions (200 μM) were prepared from the total OD_{260} of purified oligonucleotides and the extinction coefficient, ϵ_{260}, of oligonucleotides (96.4×10^3 for (GGAGCAGGAC), 81.4×10^3 for d(GTCCTGCTCC), and 83.4×10^3 for r(GUCCUGCUCC)). The non-self-complementary DNA:DNA and RNA;DNA were prepared as follows. Equal amounts of DNA:RNA and DNA strands were mixed in the 20 mM phosphate buffer (pH 7.0) containing 300 mM NaCl and then annealed at 55 °C for 3 h and cooled to 4 °C for overnight.[29] The single-stranded DNA's were prepared by mixing equal amounts of the DNA and phosphate buffer. The AMD and N8AMD solutions (10 μM) were prepared to give 0.246 absorbance at 440 and at 420 nm, respectively. After carefully determination of the base line of the spectrometer, an absorbance of 1.0 mL of drug solution (10 μM) in 20 mM phosphate buffer (pH 7.0) containing 300 mM NaCl was measured from 550 to 320 nm. A 10-μL sample of oligonucleotide, DNA:DNA or RNA:DNA, or single-stranded DNA or RNA, was added in the sample cuvette (concentration of DNA:DNA, RNA:DNA, DNA, and RNA should be 2 μM), and spectra were measured at this condition. This procedure was repeated three times so that three spectra were measured at three different DNA concentrations (2, 4, and 6 μM). In addition to these spectra, further diluted DNA spectra (DNA concentration of 0.65, 0.133, and 2.00 μM) for the AMD–DNA:DNA complex were measured in order to examine the binding constants. The absorbances of visible spectra were output at every 2-nm interval for use of the difference spectra and binding constant calculations. The difference spectra were obtained by subtracting the drug spectra from the complex spectrum after a multiplied dilution factor.

Melting Tests. A JASCO HMC-358 constant-temperature cell holder connected with a NESLAB RTE-111 bath circulator was used to measure the melting point spectra. The temperature in the cuvette was measured by putting a thermocouple directly in the cuvette. A 10-μL sample of oligonucleotide (200 μM), DNA:DNA or RNA:DNA, or single-stranded DNA, was added in the sample cuvette containing 1.0 mL of 20 mM phosphate buffer (pH 7.0) and 300 mM NaCl, and the absorption at 260 nm was measured from 15 to 70 °C. The cuvette temperature was monitored and increased at approximately 1 deg/min.

Acknowledgment. The authors express their thanks to Dr. David Huhta for his valuable instruction and suggestions in the molecular mechanics calculation and to Mrs. Li Wen for DNA synthesis and purification. We also thank Professor Richard L. Schowen for critical reading of the manuscript and valuable comments. This work has been supported by grants from the NIH, the Kansas Health Foundation, and the Marion Merrell Dow Foundation.

Supplementary Material Available: Text describing crystal structure analysis, figures showing molecular structures, and listings of atomic coordinates and equivalent isotropic thermal parameters for **12**, **14a**, **20**, and **19′** (25 pages); tables of observed and calculated structure factors (71 pages). This material is contained in many libraries on microfiche, immediately follows this article in the microfilm version of the journal, and can be ordered from the ACS; see any current masthead page for ordering information.

(38) Cromer, D. T.; Waber, J. T. In *International Tables for X-ray Crystallography*; Ibers, J. A., Hamilton, W. C., Eds.; The Kynoch Press: Birmingham, England, 1974; Vol. IV, pp 99–101, 149–150.

(39) Takusagawa, F. *Crystallographic Computing System*: KUDNA; The University of Kansas: Lawrence, KS, 1984.

(40) TEXSAN Structure Analysis Package, Molecular Structure Corporation, 1985.